NASA Technical Memorandum 102722

DETERMINATION OF THE PRESSURE DRAG OF
AIRFOILS BY INTEGRATION OF SURFACE PRESSURES

WILLIAM H. PHILLIPS

OCTOBER 1990

Introduction

The prediction of forces acting on a body in a fluid has been the subject of study by scientists and mathematicians for many centuries. In 1744, D'Alembert proved that the force on a body moving in an inviscid fluid is zero. This result puzzled scientists for many years and is known as D'Alembert's paradox. It was known that a fluid exerted forces on a body in practice, yet air was known to be a fluid of very low viscosity for which the assumption of inviscid flow should apply with good accuracy. In 1903, Ludwig Prandtl published his famous paper that introduced the concept of the boundary layer (ref. 1). In this report, he showed that the effects of viscosity were confined to a narrow layer near the body. In 1910, Prandtl stated that the forces on a two-dimensional airfoil could be divided into friction drag, resulting from forces tangential to the surface and pressure drag, resulting from forces normal to the surface (ref. 2). Both these sources of drag were shown to result from the presence of the boundary layer. References 1 and 2 have recently been made available as NASA technical translations. Despite the early introduction of this subject by Prandtl, the study of pressure drag has been given very little attention. This neglect is partly due to the difficulty of separating the drag into friction and pressure components experimentally, and partly to the complex calculations required to evaluate boundary layer characteristics and effects. This limitation is now partly overcome by the availability of high-speed computers.

Further discussion of some basic considerations concerning pressure drag are given by Prandtl in reference 3. In this analysis, Prandtl shows that the pressure drag of a half body (that is, a body extending downstream to infinity with parallel sides) is zero. This theorem is of importance in analyzing the pressure drag on an airfoil and its wake.

In a previous report (ref. 4), the author presents studies of the pressure drag and friction drag of airfoils using the Eppler program. In these studies, the pressure drag is obtained as the difference between the total drag and the friction drag, where the total drag is obtained from the equivalent of a momentum survey in the boundary layer at the trailing edge. The pressure drag may also be obtained by integrating the streamwise components of the pressure forces on the airfoil surface. One objective of the present studies is to compare the pressure drag obtained by this method with that obtained previously. A check of these values would be a good indication of the validity of the entire process of calculating the airfoil pressure distribution and the growth of the boundary layer along the surface.

Previous attempts to determine pressure drag by integrating the pressure forces on the airfoil have frequently given inaccurate or inconsistent results. At the beginning of this study, this problem was thought to be the result of inaccurate integration because of a lack of enough data points on the airfoil surface and inaccurate slopes of the contour, particularly in the region of the high pressure peak near the nose. For this reason, initial efforts concentrated on developing accurate numerical integration techniques and increasing the number of data points on the airfoil contour. By checking that the drag of the airfoil in inviscid flow is zero, the accuracy of the integration may be verified.

A second objective of the present studies is to extend some of the calculations made in the previous report to a larger range of angle of attack, and in particular, to obtain the magnitude of the pressure drag at angles of attack close to the stall.

An underlying objective of all the studies reported herein is to try to obtain a physical explanation of the cause of pressure drag on an airfoil and possibly to determine whether this component of drag may be reduced by suitable design. The author is not a specialist in this field and it is realized that many more sophisticated studies have been made involving calculation of pressure drag. The studies reported herein may be considered as part of an educational process on airfoil theory for the author and may therefore be of interest mainly to other nonspecialists who may wish to obtain an introduction to this field.

Symbols

C chordwise force

c airfoil chord

C_C chordwise force coefficient, $\dfrac{C}{1/2\rho V_\infty^2 c}$

C_D drag coefficient, $\dfrac{D}{1/2\rho V_\infty^2 c}$

C_L lift coefficient, $\dfrac{L}{1/2\rho V_\infty^2 c}$

C_N normal force coefficient, $\dfrac{N}{1/2\rho V_\infty^2 c}$

C_p pressure coefficient, $\dfrac{p}{1/2\rho V_\infty^2}$

D drag

L lift

N normal force

p pressure on airfoil surface

R Reynolds number

V_∞ free-stream velocity

x distance along chord line, positive rearward

y distance normal to chord line, positive upward

x_1 distance parallel to flow direction at infinity, positive rearward

y_1 distance normal to flow direction at infinity, positive upward

v velocity

α angle of attack with respect to zero lift line

ρ air density

Subscripts

P   pressure

T   total

fr   friction

Analysis Tools

The calculations of airfoil pressure distribution and boundary layer development are made using the Eppler program (refs. 5 and 6). The previous studies of reference 4 used only the programs of reference 5, in which the pressure distribution on the airfoil is calculated in inviscid flow, and the boundary layer development is calculated based on this pressure distribution. The procedure described in reference 6 allows the pressure distribution to be recalculated assuming that the airfoil contour is shifted by the displacement thickness of the boundary layer. This procedure gives an approximation to the pressure distribution as influenced by the boundary layer on the airfoil, which is obviously necessary in order to obtain a value for the pressure drag by integrating the surface pressures, inasmuch as the pressure drag in inviscid flow is zero.

Although the programs of reference 5 give the variation of friction drag along the surface of the airfoil, the total friction drag is not given. A separate program was written to accept the friction drag output of the Eppler program and to plot and integrate these curves to obtain the friction drag. This analysis is described in reference 4. In the present study, similar auxiliary programs were written to accept the pressure distribution on the airfoil on the original or displaced contour and to integrate these values to obtain the normal force, chord force, lift, and drag.

Cases Studied

The airfoils used in most of the present studies were the Eppler 214 (designated E-214) and the 1098. Ordinates for these airfoils are given in reference 4. In addition, a series of four symmetrical airfoils was designed in order to study the effects of thickness with zero camber. These airfoils, produced by the design method of reference 5, are designated SP-1 through SP-4. Since these airfoils have no immediate practical application, the ordinates are not given, but the TRA1 and TRA2 cards defining these airfoils in the Eppler program are given in table 1, so that these airfoils can be reproduced by the Eppler program if desired. Drawings of all the airfoils, with their inviscid pressure distributions, are given in figure 1.

Calculation of Pressure Drag by Integration of Surface Pressures

As shown in various textbooks on aerodynamics (ref. 7, for example), the coefficients of normal force, chordwise force, lift, and drag on an airfoil may be obtained from the distribution of surface pressures by the following formulas:

$$C_N = \oint C_p dx$$
$$C_C = \oint C_p dy$$

where the integration is performed around the airfoil contour. Then

$$C_L = C_N \cos\alpha - C_C \sin\alpha$$

$$C_D = C_N \sin\alpha + C_C \cos\alpha$$

In performing the integration in the present report, the pressure is assumed to be constant through the boundary layer and to be applied at the same x location on the airfoil as on the edge of the displaced contour. The pressure on the rear of the displaced contour, which is cut off square at the trailing edge, is neglected.

A slight change in this procedure is used in preparing one of the subsequent figures that shows plots of pressure components that may be integrated to obtain lift and drag coefficients directly. The values of C_N and C_C given previously are equal to the values of C_L and C_D at zero angle of attack. In order to obtain plots that can be integrated to give C_L and C_D at other values of angle of attack, the x and y locations of each point on the airfoil must be expressed with respect to axes parallel and perpendicular to the flow direction. The axes are defined as shown on the accompanying sketch:

Then
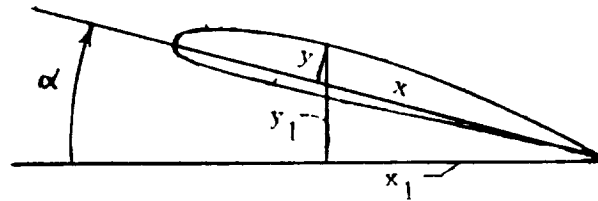
$$x_1 = x \cos\alpha + y \sin\alpha$$

$$y_1 = -x \sin\alpha + y \cos\alpha$$

Using the same integration formulas as previously:

$$C_L = \oint C_p dx_1$$

$$C_D = \oint C_p dy_1$$

Results of Calculations

Data for the 1098 and E-214 airfoils at a Reynolds number of 30 million are shown in figure 2. In this case, the pressure drag from integration of the surface pressures is omitted. The main purpose of this figure is to extend these data for these cases given in reference 4 to the stall.

The effect of changing the number of points defining the airfoil contour is shown in figure 3. Data are shown for the 1098 airfoil with 60 points and with 108 points. The drag values in figure 3 are plotted to an unusually large scale to show the effects of small errors. Note that a change in drag coefficient of .0001 (so-called one count) is usually considered to be about the smallest change that can be detected in a wind tunnel.

Comparison of values of pressure drag in inviscid flow for two integration procedures, the trapezoidal and spline methods, are given in figure 4. Data are shown for the 1098 and E-214 airfoils. Inasmuch as the total drag, pressure drag, and friction drag in inviscid flow are all zero, the occurrence of a drag value indicates an error either in the pressure distribution, the airfoil shape, or the integration procedure. In comparing two integration procedures, however, the pressure distribution and airfoil shape are identical, so that the effect of the integration procedure should be correctly shown. For these calculations, the airfoil contour was defined by 108 points, the largest number used in the study. Again, the results are plotted to a large scale.

The calculated variation of drag with angle of attack for the 1098 and E-214 airfoils at a Reynolds number of 3 million are shown in figure 5. Data are shown for the total drag, the pressure drag as obtained from the difference between the total drag and friction drag, and the pressure drag obtained by integrating the surface pressures. These results have been extended somewhat to higher angles of attack than those shown in reference 1 in order to reach the stall.

The calculated variation of drag with angle of attack for the four symmetrical airfoils, SP-1 to SP-4 at a Reynolds number of 3 million, are given in figure 6. Again, the total drag and the pressure drag obtained by the two methods are given.

Examples of plots of the surface pressure versus the x and y coordinates, which are integrated to get the normal and chordwise force coefficients, are shown in figure 7 for the case of the SP-4 airfoil at angles of attack of 0° and 8°, This case of an extremely thick airfoil (which is not exact because of the existence of a separated region on the upper surface near the trailing edge) is shown in order to allow the differences between the inviscid and iterated cases to be seen. The boundary layer development in the separated region is only roughly approximated in the Eppler program.

Discussion of Results

The data of figure 2 show the total drag and pressure drag of the E-214 and 1098 airfoils at a Reynolds number of 30 million, with the pressure drag calculated as the difference between total drag and friction drag. The main purpose of this figure is to extend the results in reference 4 to the stall, and thereby to show how large the pressure

drag may become at angles of attack near the stall. In the case of the 1098 airfoil, the stall occurs gradually as separation progresses forward from the trailing edge. At an angle of attack of 18°, where the separation has reached 0.2 chord ahead or the trailing edge, the pressure drag has reached 69 percent of the total. Values are not considered reliable at higher angles of attack because separated flow is only roughly approximated in the Eppler program. In the case of the E-214 airfoil, the pressure drag is 76 percent of the total just below the stall.

The subject of calculation of drag by integration of surface pressures is now considered. The effect of changing the number of points defining the airfoil from 60 to 108, as shown in figure 3, appears to be important, particularly at high angles of attack. For example, the value of the pressure drag in inviscid flow is reduced from 11 counts to 5 counts at an angle of attack of 12° by use of the larger number of points. The indication is that still more points would be beneficial. The value of 5 counts is small enough compared to the actual pressure drag at 12° angles of attack (about 50 counts), that it does not invalidate the results of the studies reported herein.

As shown in figure 4, the difference between the values of pressure drag obtained using trapezoidal integration and spline integration is very small, generally of the order of 1 count. The conclusion may be reached that errors introduced by the integration procedure are not responsible for large errors previously noted in obtaining pressure drag by integration of the surface pressures. Inasmuch as the spline integration procedure fits the pressure distribution plots more accurately, it was used in obtaining the results presented subsequently.

The main results of this investigation, showing the comparison of pressure drag obtained by two methods, are given in figures 5 and 6. As shown in figure 5, the pressure drag obtained by integration of the surface pressures for the 1098 and E-214 airfoils is much less than that obtained as the difference between total drag and friction drag, despite the fact that the integration procedure has been shown to be sufficiently accurate. The pressure drag obtained as the difference between total drag and friction drag is believed to be reasonably accurate, as well as consistent with the total drag, because both the friction drag and total drag depend on the boundary layer development along the entire airfoil surface. In other words, a localized variation in boundary layer thickness, such as due to separation near the trailing edge, would not have any large effect on the integrated friction drag. The discrepancy between the two methods is therefore believed to be primarily due to errors in the pressure drag obtained by integration of the surface pressures.

The question arises as to where the error appears in the distribution of surface pressures. In the past, these errors have occurred whether the pressure data were experimental or theoretical. Frequently, these errors have been blamed on insufficient accuracy in defining the pressures near the leading edge of the airfoil, where the pressures are large and the surface slopes are changing rapidly. The results of figures 3 and 4 show, however, that, at least in the case where the pressures are computed theoretically, sufficient accuracy is obtained with the calculation and integration procedures.

In order to show the effect of airfoil thickness on the calculation of pressure drag, without the complicating effect of camber, the symmetrical airfoils SP-1 and SP-4 were studied. These results are shown in figure 6. In the case of the thinnest airfoil, SP-1, with a thickness of 4.73 percent, good agreement is shown between the values of pressure drag

as calculated by the two methods. This case is the only one, however, in which this agreement is shown. As the airfoils become thicker, the pressure drag obtained by integrating the surface pressures becomes progressively lower as compared to the value obtained from the difference between total drag and friction drag. In the case of airfoils SP-3 and SP-4, 19.5 and 26.7 percent thick, respectively, the pressure drag obtained by integrating the surface pressures becomes negative.

The occurrence of negative values of pressure drag is in disagreement with the results obtained from the difference between total drag and friction drag, and is contrary to experimental evidence. Previous investigators have found that the inviscid pressure distribution of an airfoil has a larger increase at the trailing edge than that occurring in the actual flow, and as a result, the boundary layer in the vicinity of the trailing edge based on this pressure distribution increases in thickness more rapidly than in the actual flow. The pressure distribution based on this displaced contour influences the pressure on the rear part of the airfoil, resulting in reduced pressure drag.

In order to illustrate this effect, the displaced contour of the SP-4 airfoil and the pressure distribution based on the first iteration of the boundary layer are shown in figure 7 for angles of attack of 0° and 8°. The SP-4 airfoil, with its large thickness, may result in inaccurate results because of separated flow at the trailing edge, but it is used as an illustration because the effects on the displaced contour and on the pressure distributions are large enough to see on the plots. In figure 7a, for an angle of attack of 0°, the horn-shaped divergence of the displaced contour at the trailing edge is visible. This contour produces a slightly increased pressure all along the rear half of the airfoil. This seemingly small change is enough to produce the negative pressure drag noted previously. Integration of the area of the plot of C_p versus y/c produces the chord force coefficient, which at zero angle of attack is the same as the drag coefficient. The integration for the inviscid case gives a value near zero, as it should. The loop near y/c = 0, containing the stagnation point region, gives a rearward force, whereas the loop at higher values of y/c gives a forward force. The area of this loop is increased slightly for the displaced contour. This difference is enough to account for the negative value of pressure drag shown in figure 6. Note that for zero angle of attack, the plot is symmetrical about y/c = 0. Eppler, in reference 6, noted the excessive increase of boundary layer thickness at the trailing edge, and made provisions in the program to arbitrarily limit the rate of growth of the boundary layer in this region in order to conform more closely to the true rate of growth. A limit is applied to the curvature of the variation of the boundary layer displacement thickness with x (that is, $d^2 \delta_1/dx^2$). The limit is preset to 1.0 in the program of reference 5. Attempts to use lower values of this limit showed that in the case of the SP-3 and SP-4 airfoils, the negative values of pressure drag were decreased, but appeared to approach zero rather than positive values.

In figure 7b, similar results are shown for an angle of attack of 8°. As may be seen, the lift coefficient is reduced somewhat, but not enough to agree with experiment. The increased positive pressure (or reduced negative pressure) on the upper surface of the airfoil reduces both the forward and rearward loops in the plot that is integrated to obtain drag coefficient, but the net effect is a negative pressure drag shown in figure 6.

The effect of the adverse gradient near the trailing edge in inviscid flow is discussed more fully in references 6, 8, and 9. In reference 6, Eppler states that the method is not extended beyond the first iteration because subsequent iterations would diverge, a problem discussed more fully in reference 9. Eppler, as mentioned previously, also provides a

method to reduce arbitrarily the rate of growth of the boundary layer near the trailing edge in order to conform more closely to the true boundary layer growth. The discussion in reference 8 shows that steps must be taken to insure continuity of the boundary layer at the trailing edge with the wake in order to obtain a more accurate representation of the flow in the vicinity of the trailing edge. A historical account of studies of this problem is given in reference 9, which discusses methods of stabilizing the iteration procedure and of providing continuity of the boundary layer with the wake at the trailing edge. Even with these more complex methods to represent the flow, the integration of surface pressures to determine pressure drag is found to be inaccurate. In references 9, it is concluded that the most accurate way to determine total drag is by a momentum integral at the trailing edge, and that the pressure drag may then be determined by subtraction of the surface friction, as was done in reference 4.

The conclusion is indicated that the pressure drag is very sensitive to conditions near the trailing edge, and that errors in the boundary layer calculation in the vicinity of the trailing edge are responsible for the poor accuracy of the pressure drag obtained by integration of the surface pressures.

Physical Explanation of Pressure Drag

The simplest case to consider is that of a symmetrical airfoil at zero lift. The theorem given by Prandtl in reference 3 states that the pressure drag of a half body extending to infinity with parallel sides is zero. This theorem may be used to give some insight into the existence of a pressure drag on such an airfoil. Consider the airfoil with its associated boundary layer and wake, as shown in figure 8. The boundary of the wake is that associated with its displacement thickness. Because the flow at the centerline of the wake accelerates from zero velocity at the trailing edge to free stream velocity at infinity, the displacement boundary converges and has a concave contour near the trailing edge. As a result, the pressure on this boundary is increased above that existing without the boundary layer, and has a forward component. There is therefore a net thrust force on the wake boundary, and a corresponding drag on the contour of the boundary layer around the airfoil. According to reference 8, this concept has been used by some investigators to calculate the pressure drag.

The pressures exerted on the outer edge of the boundary layer may be expected to be transmitted to the airfoil contour, but the airfoil contour on the average has more converging slope, so that these pressures would exert a different force on the airfoil than on the edge of the boundary layer. The pressure drag on the airfoil itself may therefore be expected to be different from the drag of the outer edge of the contour, the difference serving to accelerate the boundary layer forward or rearward. Presumably, these effects are very small.

The case of the lifting airfoil is more complex. The data of the present report and of reference 4 show that the pressure drag increases rapidly with increasing angle of attack. Probably, the greatest contribution to the pressure drag comes from the fact that the airfoil is tilted to a higher angle of attack to produce the lift than would be required in inviscid flow. This difference is caused by the effect of the boundary layer on the Kutta condition at the trailing edge. Inasmuch as the pressures on the contour are transmitted to the airfoil without much change, but act on an airfoil surface that is tilted to a higher angle of attack, a

rearward component of lift is produced equal to $C_N\Delta\alpha$. If the lift coefficient is 1, for example, and the lift curve slope is 95 percent of its inviscid value of about 2π, the pressure drag produced would be .008. In addition to this effect of the tilted lift vector, the effects described for the symmetrical airfoil at zero lift are still present.

It is interesting that the pressure drag is easiest to visualize by considering effects in the wake, yet the drag itself is the result of normal and tangential forces on the surface of the airfoil. The laws of nature arrange for the boundary layer, which results from forces all along the airfoil contour, to have a profile at the trailing edge that sets the circulation and allows all the momentum relations to be satisfied. A simple physical understanding of this process appears impossible to obtain as it involves the interaction of the airfoil with the entire flow field.

Concluding Remarks

The present studies, as well as previous investigations, show that the pressure drag of an airfoil in incompressible flow is a relatively large percentage of the total drag, reaching 60 to 80 percent of the total drag at angles of attack near the stall. Further studies to determine the sources of pressure drag and methods to reduce the pressure drag are therefore desirable.

The results of calculations using the Eppler program show that the pressure drag obtained by integration of the surface pressures on the airfoil with the contour displaced by the boundary layer thickness based on the inviscid pressure distribution is seriously in error. The source of error is not the lack of sufficient points on the contour, or the integration procedure itself, as shown by the fact that the pressure drag in inviscid flow is sufficiently close to zero.

The source of error in the pressure drag calculations is believed to be the inaccuracy in the calculation of the boundary layer development in the region of the trailing edge, and in the failure to include the influence of the wake on the pressures in this region. Studies by other investigators have shown the importance of these effects.

The method of calculating the pressure drag as the difference between total drag, obtained from a momentum integral at the trailing edge, and friction drag, is relatively insensitive to errors in the flow conditions at the trailing edge, and therefore gives reasonably reliable results. Nevertheless, the failure of the integration of surface pressures to give pressure drag in agreement with the difference method indicates that the Eppler program using the first iteration of the displaced airfoil contour is not completely self consistent and that some errors may exist in the lift and drag obtained by this method.

In view of the complex nature of the flow near the trailing edge, particularly in cases in which boundary layer separation occurs, there does not appear to be any simple method to calculate the magnitude of the pressure drag, or any simple physical explanation of its occurrence.

References

1. Tolmien, W.; Schlichting, H.; and Goertler, H.: Ludwig Prandtl Collected Treatises on Applied Mechanics, Hydro- and Aerodynamics, Part 2, IV, Interfaces and Resistance. NASA TT-20315: (Translated from L. Prandtl: The Motion of Liquid When Very Slight Friction is Present. Proceedings of the Third International Congress of Mathematicians, Heidelberg, 1904, pp. 484-491: Teubner 1905.)

2. Tolmien, W.; Schlichting, H.; and Goertler, H.: Ludwig Prandtl Collected Treatises on Applied Mechanics, Hydro- and Aerodynamics, Part 1. NASA TT-20316, pp. 28-48: (Translated from L. Prandtl: Some Remarks on Air Resistance. Zeitschrift fuer Flugmechanik und Motor Luftschiffahrt, 1 (1910), pp. 73-76.)

3. Prandtl, L.: The Mechanics of Viscous Fluids. Aerodynamic Theory, W. F. Durand, Editor. Vol. III, Division G., January 1943, pp. 190-197.

4. Phillips. W. H.: Studies of Friction Drag and Pressure Drag of Airfoils Using the Eppler Program. SAE Technical Paper 881396, presented at Aerospace Technology Conference and Exposition, Anaheim, California. October 3-6, 1988. (Also in Advanced Aerospace Aerodynamics, SAE Publication SP-757, pp. 71-86.)

5. Eppler, R.; and Somers, D. M.: A Computer Program for the Design and Analysis of Low-Speed Airfoils. NASA TM-80201, August 1980.

6. Eppler, R.; and Somers, D. M.: Supplement to: A Computer Program for the Design and Analysis of Low-Speed Airfoils. NASA TM-81862, December 1980.

7. Rauscher, M.: Introduction to Aeronautical Dynamics. John Wiley and Sons, Inc., New York, Chapman and Hall, Ltd., London, 1953, pp. 330-332.

8. Smith, A. M. O.; and Cebeci, T.: Remarks on Methods for Predicting Viscous Drag. AGARD-CP-124, AGARD Conference Proceedings No. 124 on Aerodynamic Drag, Paper No. 7, April 1973.

9. Lock, R. C.: Prediction of the Drag of Wings at Subsonic Speeds by Viscous/Inviscid Interaction Techniques. AGARD-R-723, AGARD Report No. 723, Aircraft Drag Prediction and Reduction, Paper No. 10, July 1985.

TABLE 1

TRA1 and TRA2 cards for symmetrical airfoils SP-1 through SP-4. These cards define the airfoil in the Eppler design program (reference 5).

Airfoil SP-1

```
TRA1 8165 2750 200 2900 400 000 1000 3100-1000 3250 -400 6000 -200 000 000
TRA2 8165  400 1450 200-1000 940 400 1450 200-1000 940  300  400
```
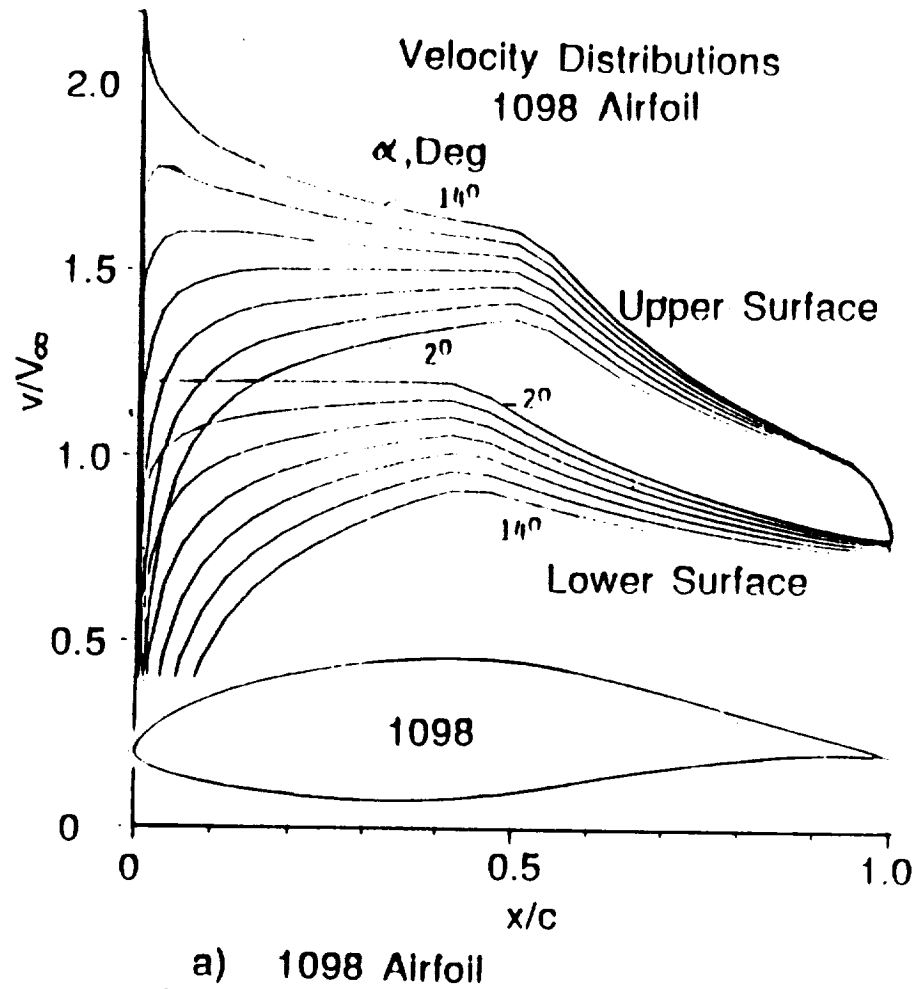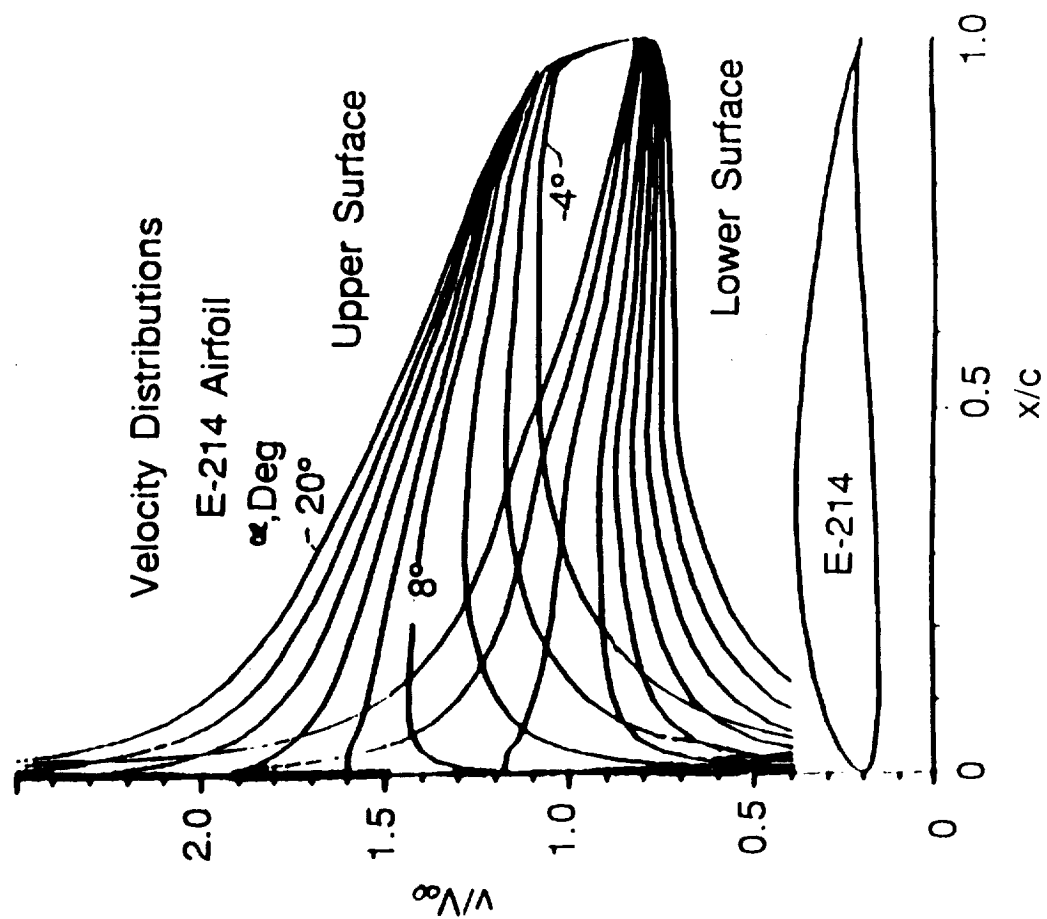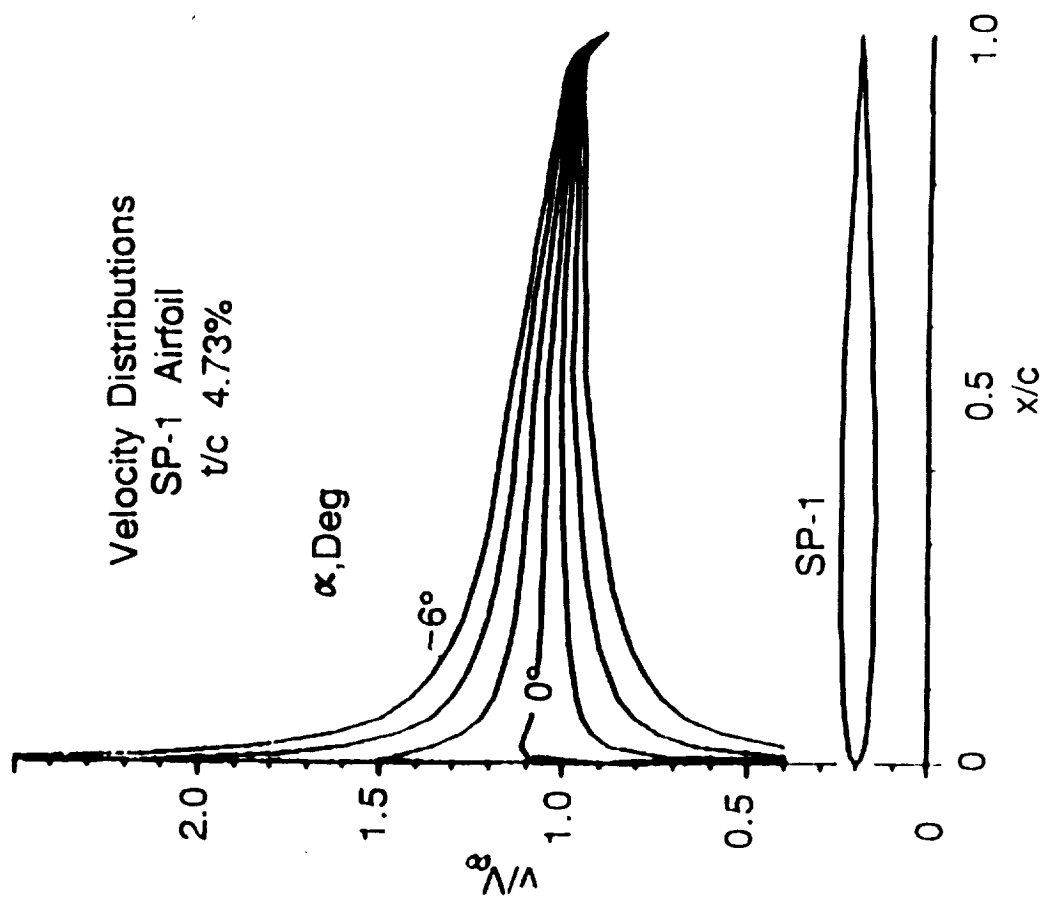
Airfoil SP-2

```
TRA1 8163 2750 200 2900 400 000 1000 3100-1000 3250 -400 6000 -200 000 000
TRA2 8163  400 1450 200-1000 000 400 1450 200-1000 800  300  400
```

Airfoil SP-3

```
TRA1 8161 2750 200 2900 400 000 1000 3100-1000 3250 -400 6000 -200 000 000
TRA2 8161  400 1450 200-1000 616 400 1450 200-1000 616  300  400
```

Airfoil SP-4

```
TRA1 8164 2750 200 2900 400 000 1000 3100-1000 3250 -400 6000 -200 000 000
TRA2 8164  400 1450 200-1000 500 400 1450 200-1000 500  300  400
```

a) 1098 Airfoil

Figure I. - Airfoils studied, and their inviscid pressure distributions.

b) Eppler 214 airfoil

Figure I. - Continued

Velocity Distributions
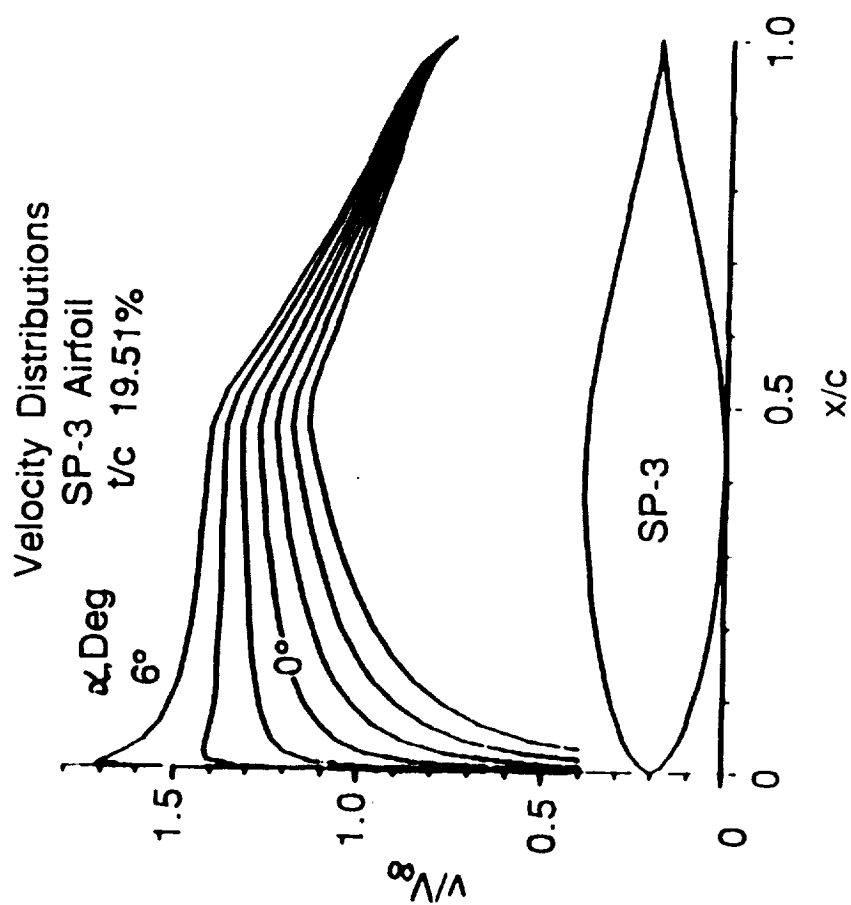SP-1 Airfoil
t/c 4.73%

c) SP-1 Airfoil

Figure l. - Continued

Velocity Distributions
SP-2 Airfoil

α, Deg

6°

0°

V/V_∞

2.0

1.5

1.0

0.5

SP-2

0

0.5
x/c

1.0

0

d) SP-2 Airfoil

Figure I. - Continued

Velocity Distributions
SP-3 Airfoil
t/c 19.51%

α,Deg
6°

0°

V/V_∞

1.5

1.0

0.5

0

0.5

1.0

x/c

SP-3

e) SP-3 Airfoil

Figure I. - Continued

Velocity Distributions
SP-4 Airfoil
t/c 26.72 %
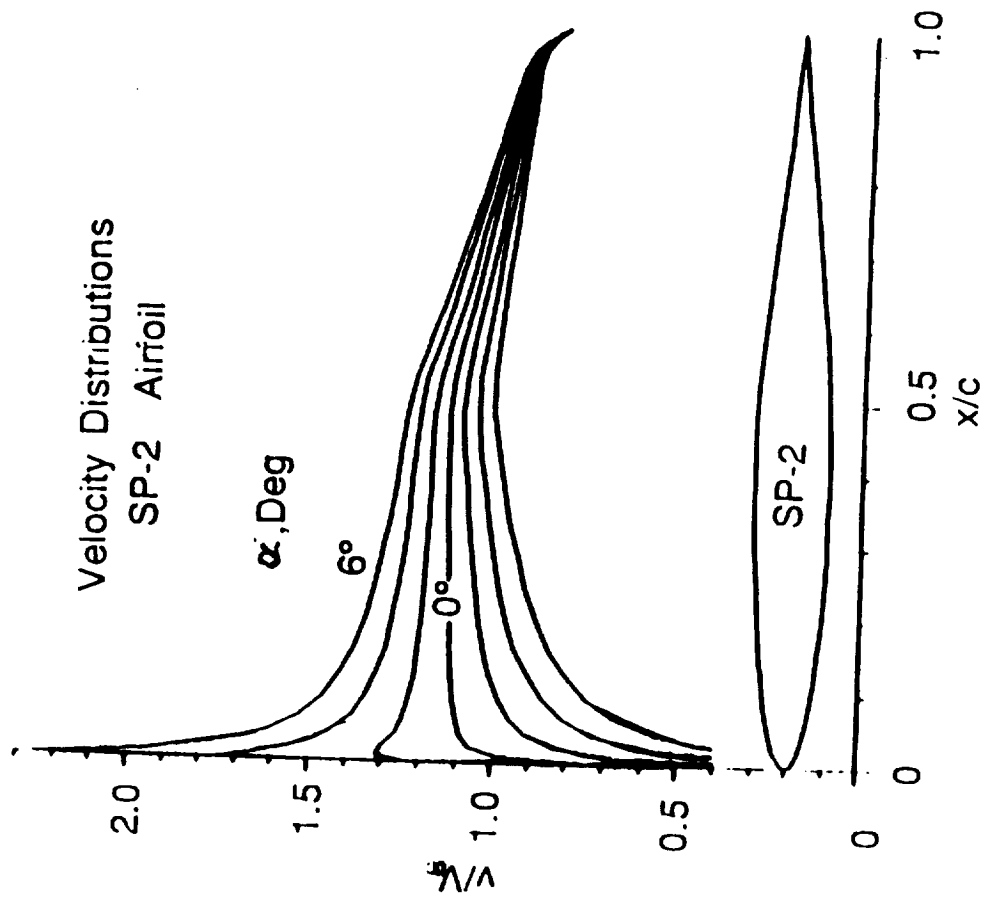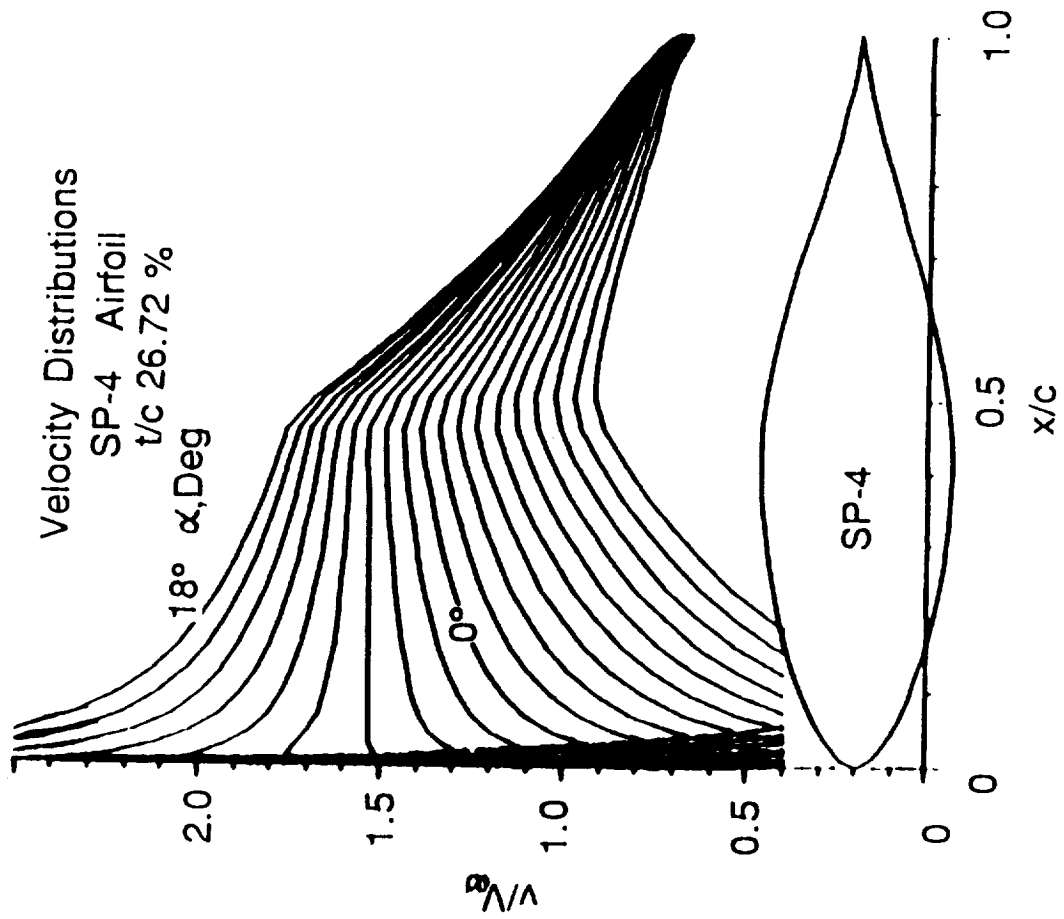
f) SP-4 Airfoil

Figure I. - Concluded
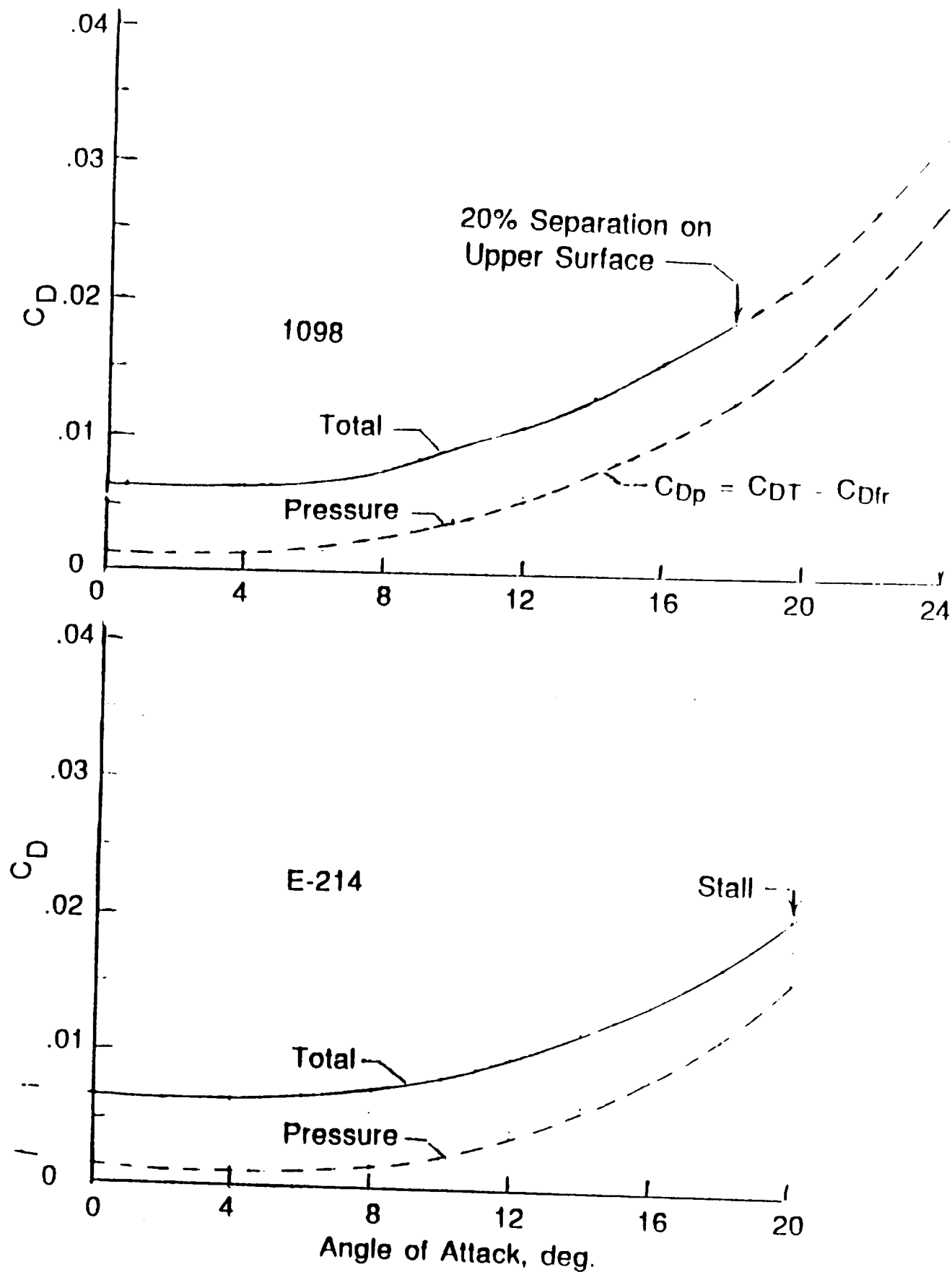
Figure 2. - Total drag and pressure drag as functions of angle of attack for a Reynolds number of 30 million.
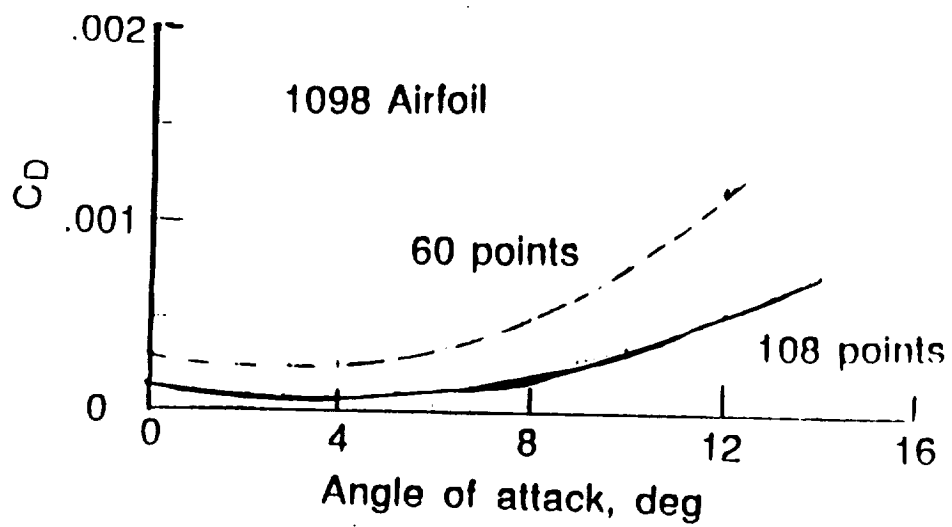
Figure 3. - Effect of number of points on the airfoil contour on calculated drag in inviscid flow. Note expanded drag scale.
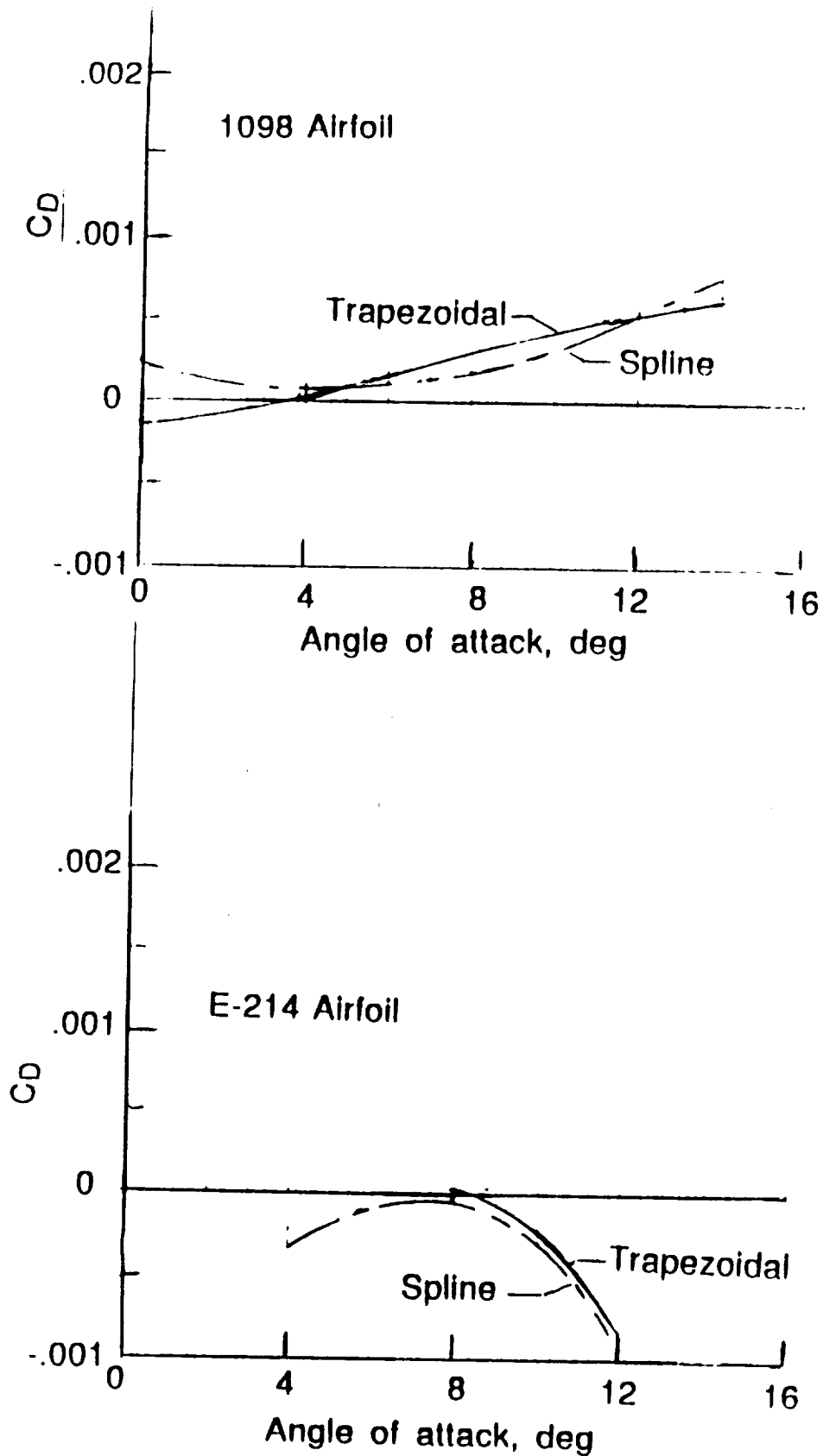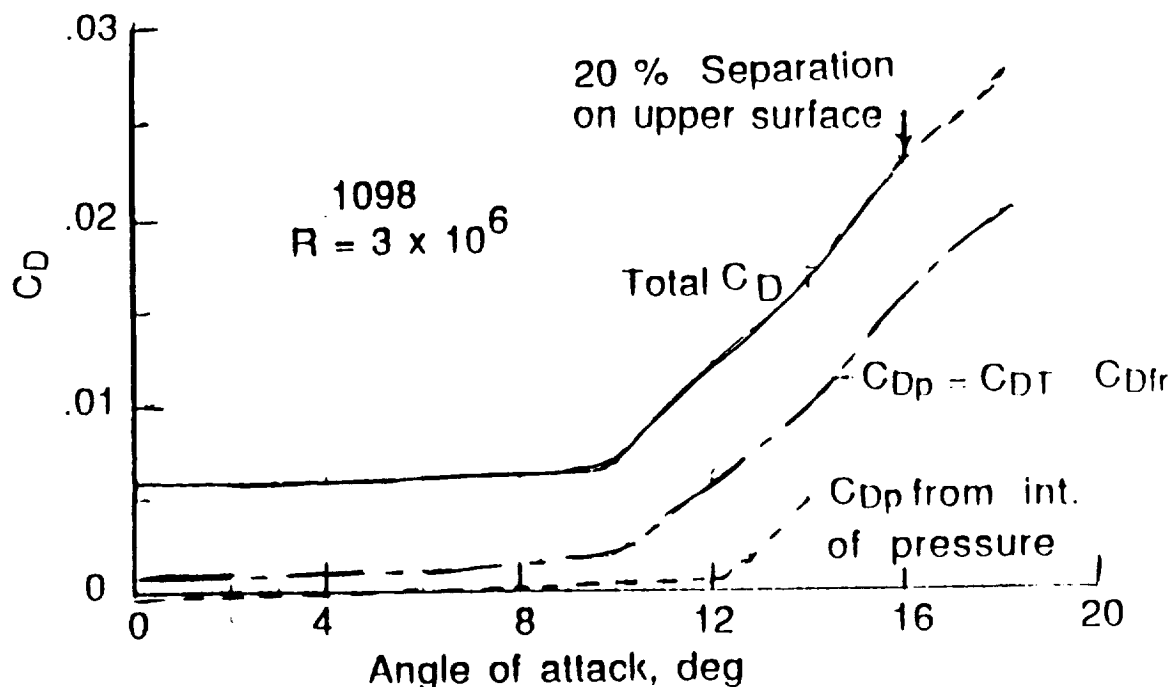
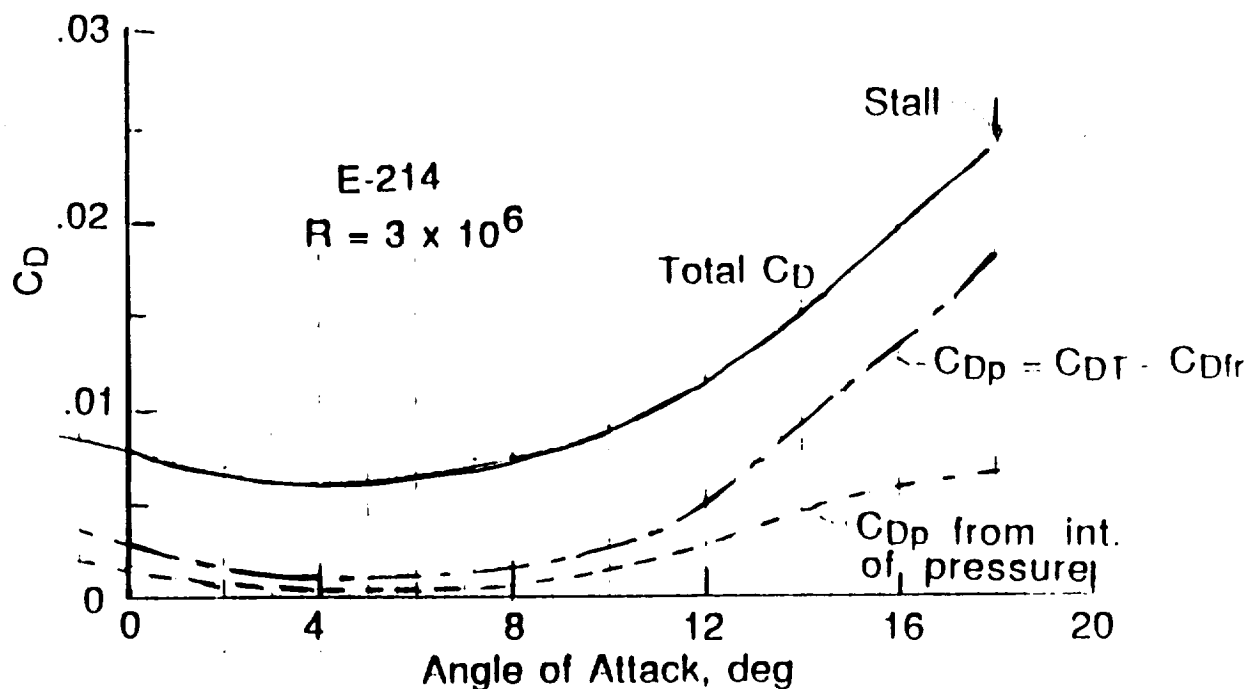Figure 4. - Effect of type of Integration on calculated drag in inviscid flow. Note expanded drag scale.

.03

C_D

20 % Separation
on upper surface ↓

1098
$R = 3 \times 10^6$

.02

Total C_D

.01

$C_{Dp} = C_{DT} - C_{Dfr}$

C_{Dp} from int.
of pressure

0

0   4   8   12   16   20

Angle of attack, deg

a) 1098 Airfoil

.03

C_D

Stall ↓

E-214
$R = 3 \times 10^6$

.02

Total C_D

$C_{Dp} = C_{DT} - C_{Dfr}$

.01

C_{Dp} from int.
of pressure

0

0   4   8   12   16   20

Angle of Attack, deg

b) E-214 Airfoil

Figure 5. - Total drag and pressure drag as functions
of angle of attack for a Reynolds number of 3 million.
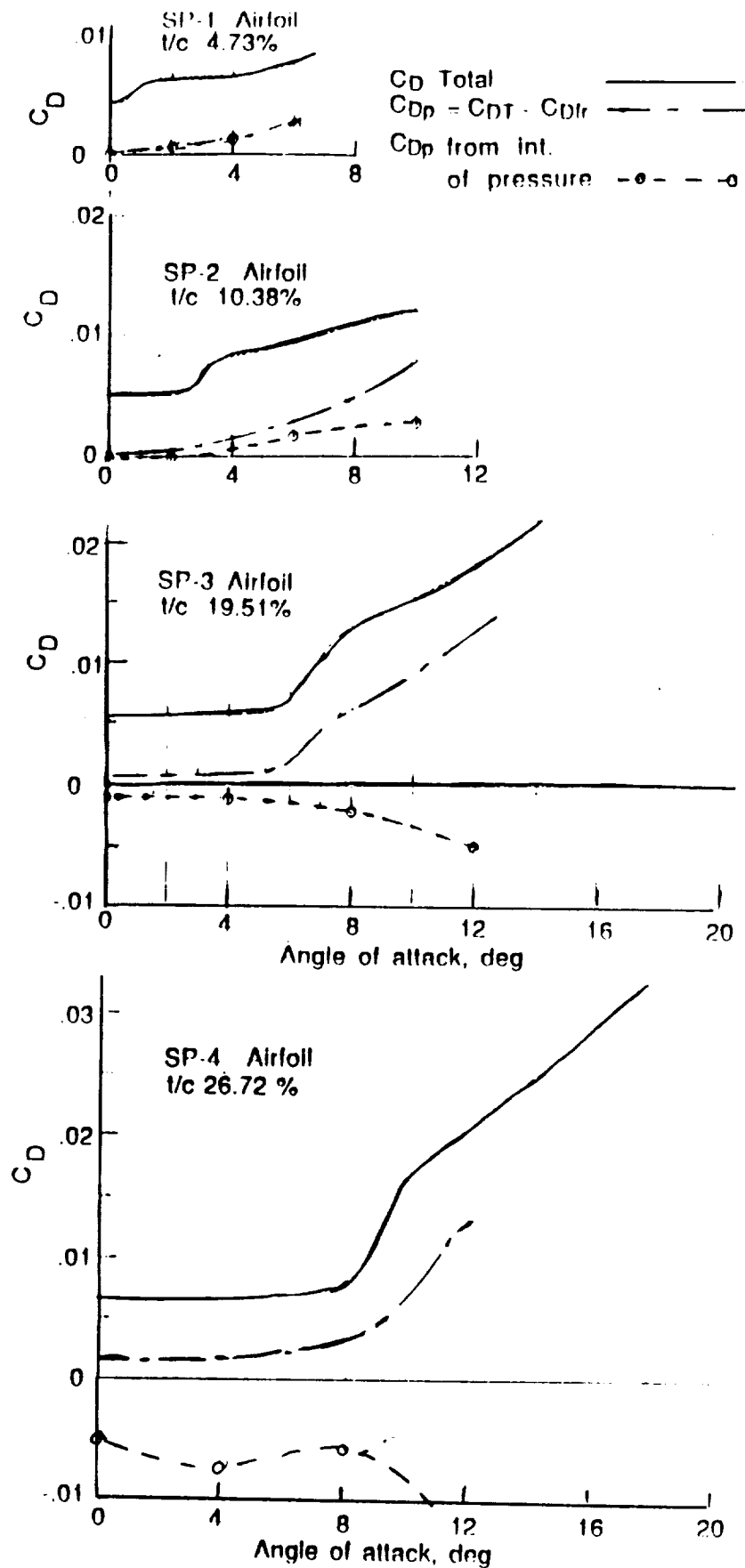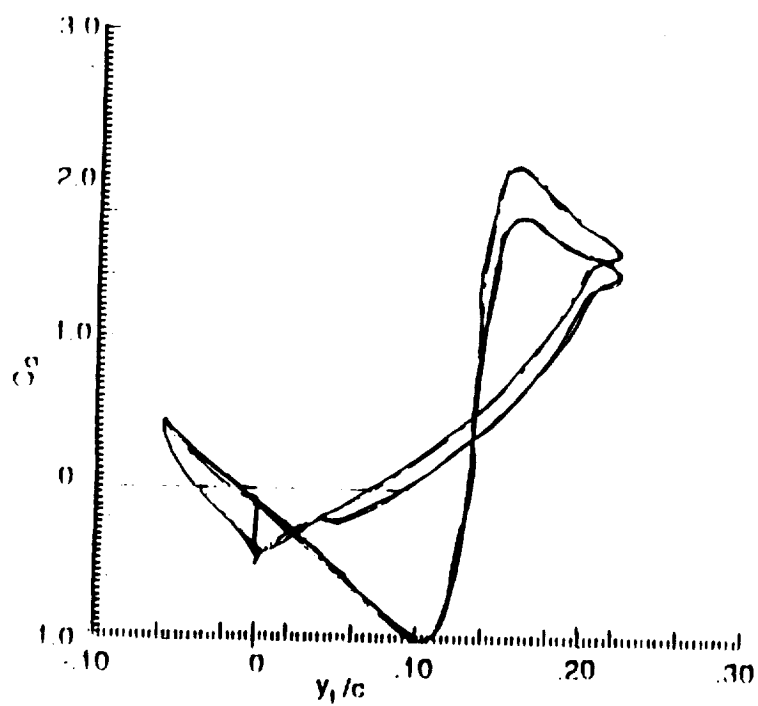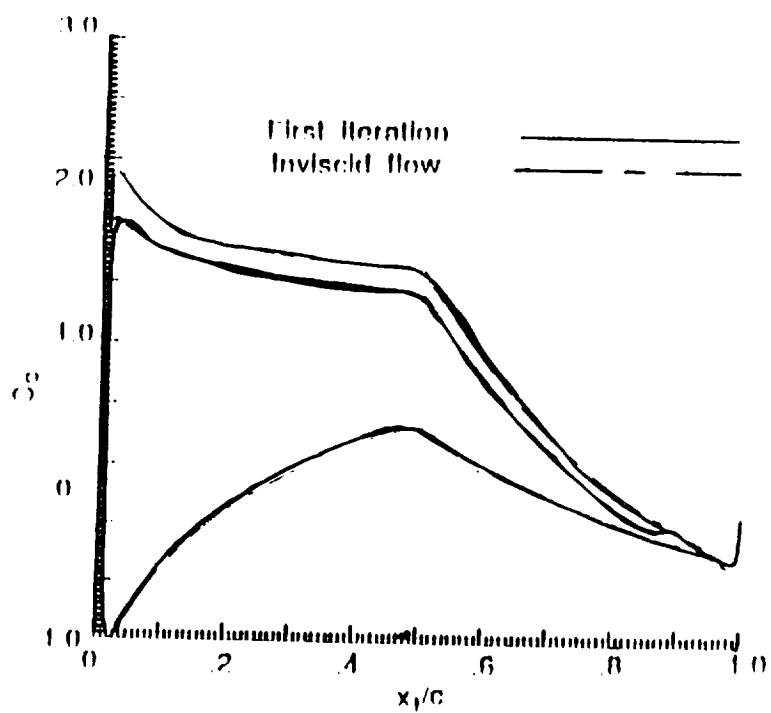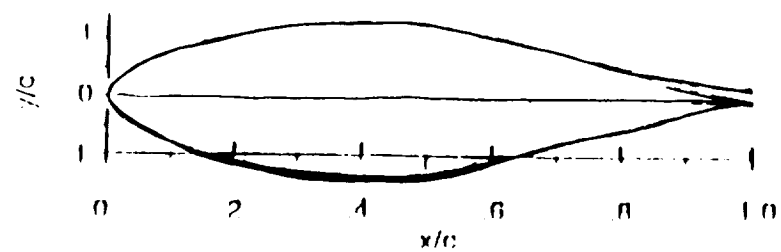Pressure drag obtained by two methods.

Figure 6. - Total drag and pressure drag as functions of angle of attack for a series of symmetrical airfoils. $R = 3 \times 10^6$. Pressure drag obtained by two methods.

b) $\alpha = 8°$

Figure 7. - Concluded

Displacement boundary of
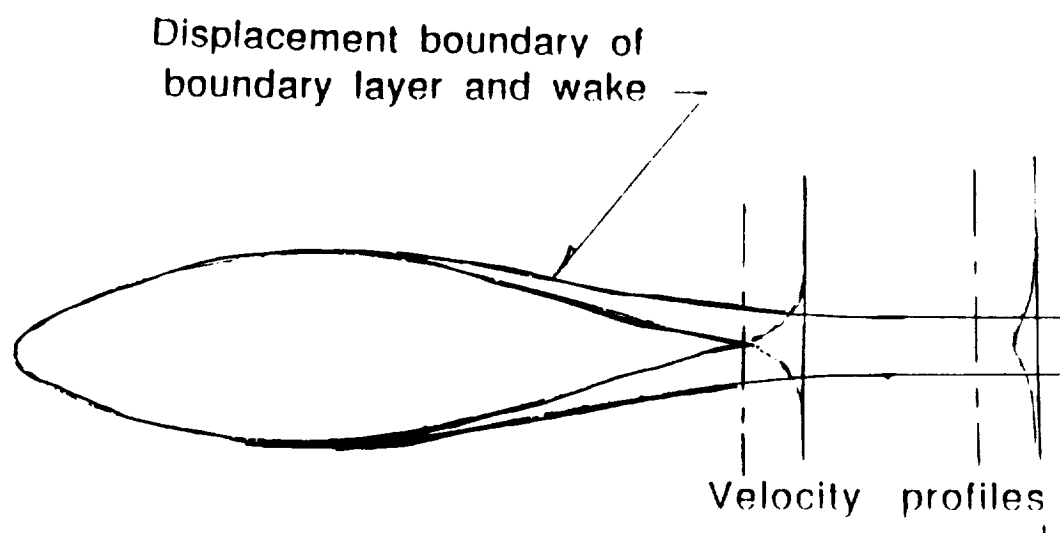boundary layer and wake

Velocity profiles

Figure 8. - Symmetrical airfoil at zero angle of attack, showing convergence of displacement boundary aft of trailing edge (exaggerated).

Report Documentation Page

1. Report No.	2. Government Accession No.	3. Recipient's Catalog No.
NASA TM-102722		

4. Title and Subtitle	5. Report Date
Determination of the Pressure Drag of Airfoils by Integration of Surface Pressures	October 1990
	6. Performing Organization Code

7. Author(s)	8. Performing Organization Report No.
William H. Phillips	
	10. Work Unit No.
	505-66-01-02

9. Performing Organization Name and Address	11. Contract or Grant No.
NASA Langley Research Center Hampton, VA 23665-5225	
	13. Type of Report and Period Covered

12. Sponsoring Agency Name and Address	Technical Memorandum
National Aeronautics and Space Administration Washington, DC 20546	14. Sponsoring Agency Code

15. Supplementary Notes

16. Abstract

A study has been conducted of the causes of pressure drag of subsonic airfoils. In a previous paper by the author, the pressure drag is obtained by calculating the total drag from the momentum defect in the boundary layer at the trailing edge and subtracting the friction drag obtained from integration of surface friction along the chord. In the present paper, the pressure drag is obtained by integrating the streamwise components of surface pressure around the airfoil. Studies were made to verify the accuracy of the integration procedure. The values of pressure drag were much smaller than those obtained by the previous method. This lack of agreement is attributed to the difficulty of calculating boundary-layer conditions in the vicinity of the trailing edge and to the extreme sensitivity of the circulation and lift to the trailing-edge conditions. Discussion is given comparing the results of these studies with those of previous investigations.

17. Key Words (Suggested by Author(s))	18. Distribution Statement
Pressure drag Airfoils, drag Airfoils, subsonic Airfoils, analytical studies	Unclassified - Unlimited Subject Category - 08

19. Security Classif. (of this report)	20. Security Classif. (of this page)	21. No. of pages	22. Price
Unclassified	Unclassified	25	A03